IOP PUBLISHING PLASMA PHYSICS AND CONTROLLED FUSION

Plasma Phys. Control. Fusion **49** (2007) 905–928 doi:10.1088/0741-3335/49/6/014

Nonlinear tearing mode in inhomogeneous plasma: I. Unmagnetized islands

F L Waelbroeck

Institute for Fusion Studies, the University of Texas, Austin, TX 78712-0262, USA

Received 2 March 2007, in final form 13 April 2007
Published 9 May 2007
Online at stacks.iop.org/PPCF/49/905

Abstract

A theory of the nonlinear growth and propagation of magnetic islands in the semi-collisional regime is presented. The theory includes the effects of finite electron temperature gradients and uses a fluid model with cold ions in slab geometry to describe islands that are unmagnetized in the sense that their width is less than ρ_s, the ion Larmor radius calculated with the electron temperature. The polarization integral and the natural phase velocity are both calculated. It is found that increasing the electron temperature gradient reduces the natural phase velocity below the electron diamagnetic frequency and thus causes the polarization current to become stabilizing.

(Some figures in this article are in colour only in the electronic version)

1. Introduction

Magnetic islands are observed to affect the performance of reversed-field pinches [1–5], stellarators [6–11] and tokamaks [12–16]. In stellarators and tokamaks, islands located in the confinement region bring about a significant degradation in the overall confinement due to the rapid transport of particles and heat along the magnetic field [6, 16]. The confinement within the island itself, however, has been observed to be very good in reversed-field pinches [2, 3], stellarators [10] and tokamaks [12, 15]. In the edge of stellarators, magnetic island chains have been put to advantage both as divertors [7] and as a tool to control the edge rotation and induce transitions to regimes of enhanced confinement [11]. Clearly, it is desirable to understand the effect of magnetic islands on the profiles as well as the factors that govern their growth.

An important factor in the growth of magnetic islands is the polarization current that arises when an island propagates with respect to the surrounding plasma. This current is caused by the acceleration of the plasma displaced by the propagating island. Its effect depends on the phase velocity of the island, that is, on the difference between the velocity of the island and that of the surrounding plasma. In the linear regime, the polarization current has been shown to be strongly stabilizing, leading to complete stability for $\Delta'\rho_s < \hat{\beta} f(\eta_e)$ [17–19]. Here $\hat{\beta} = 0.5\beta L_s^2/L_n^2$, β is the ratio of thermal to magnetic energy, $\eta_e = L_n/L_T$ where $L_n = -(\nabla \ln n)^{-1}$ and $L_T = -(\nabla \ln T_e)^{-1}$ are the density and electron temperature scale lengths, L_s is the magnetic shear length, Δ' describes the free energy driving the tearing mode,

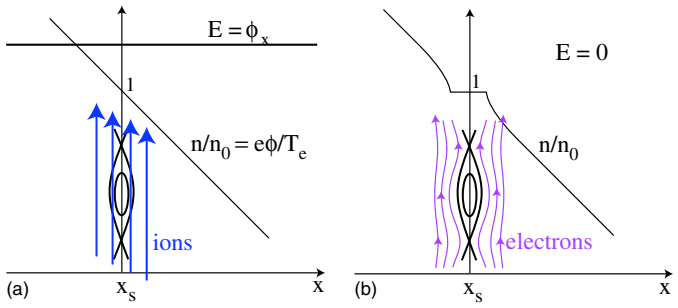

Figure 1. Sketch of the density profile and the particle velocities in the two opposing limits where the density gradient is (*a*) unaffected or (*b*) flattened inside the separatrix.

$\rho_s = c_s/\omega_{ci}$, $c_s = (T_e/m_i)^{1/2}$ is the sound speed and ω_{ci} is the ion cyclotron frequency. The factor $f(\eta_e)$, given in equations (27)–(28), describes the dependence of the stability threshold on η_e and takes positive values of order unity for $\eta_e > 0$.

In the nonlinear regime, in contrast, the role of the polarization current is incompletely understood. Its possible stabilizing effect is presently of considerable interest for predicting the stability of the neoclassical tearing mode (see [20, 21] and references therein). It is also of interest for resolving the discrepancies between the theory and the observations of magnetic healing in stellarators [22]. Early calculations of the polarization current by Smolyakov [23] using a fluid model and by Wilson *et al* [24] using the drift-kinetic equation were shown in subsequent papers to be incorrect [25–32]. These subsequent papers, however, avoided calculating the island propagation velocity, treating it instead as an input parameter. Since the sign of the polarization current depends on the island velocity, determining this velocity is necessary in order to draw conclusions regarding the effect of the polarization current on island evolution [33].

The dominant consideration in determining the island velocity is the degree of density flattening across the island. To understand the role of density flattening, we consider a plasma with constant temperature ($\eta_e = 0$) and examine the two limiting cases where the density gradient is either unaffected or entirely flattened within the separatrix (figure 1). When the density gradient is unaffected inside the separatrix, the electrons experience a diamagnetic drift. The 'frozen-in' property, however, requires that the phase velocity of the island match the electron velocity. The island will thus propagate at the electron diamagnetic velocity. In a frame moving with the island, an electric field arises such that the corresponding electric drift cancels the diamagnetic drift of the electrons, bringing them to rest inside the separatrix. The electric field balances the pressure gradient along the field lines, ensuring equilibrium. The ions stream through the island without experiencing any acceleration, carried by the electric and, for $T_i > 0$, by their diamagnetic drifts. Thus, in the limit where the density gradient is unaffected, the polarization current vanishes.

In the limit where the density is flattened within the island, in contrast, both species move at the same velocity, the electric drift velocity, inside the separatrix. The frozen-in condition requires again that the electrons (and thus the ions) be at rest with respect to the island. Outside the island, however, the background density gradient causes the ions and the electrons to flow at different velocities. Thus, the velocity of the two species must change rapidly as one moves from inside to outside the island. This change in velocity is opposed by viscosity. The velocity of the island is thus determined by the competition between electron and ion viscosity [34–36]. Since the ion viscosity ordinarily dominates, one expects the phase velocity to lag only slightly behind that of the background ions.

The conditions for density flattening have been the subject of much research. A generally accepted result due to Scott *et al* [37] is that the density is flattened by sound waves when the amplitude of the mode is such that $\omega_{*e} \sim k_\parallel c_s$, where $\omega_{*e} = k_Y \rho_s c_s / L_n$ is the diamagnetic frequency, k_Y is the azimuthal wavevector, $k_\parallel = k_Y W / L_s$ is the component of the wavevector along the magnetic field and W is the island half-width. The corresponding characteristic width for acoustic flattening is thus $W_a = \rho_s L_s / L_n$. For islands of this size fluid theory is inapplicable but one expects ion Landau damping to replace the sound wave as the mechanism of pressure flattening. This will leave the conclusions of Scott *et al* [37] unchanged. We note also that experimental observations of peaked density profiles in large islands after pellet fuelling do not contradict the sound wave model since the peaked density profiles in these islands conform to the flux surfaces [12]. That is, the density is constant along the magnetic field.

In devices with weak magnetic shear, however, such as tokamaks and stellarators, the characteristic width for acoustic flattening, W_a, is typically much greater than the ion gyroradius. It is of interest to know whether other mechanisms exist that would result in a smaller threshold for density flattening than that predicted by the sound wave mechanism. Ottaviani *et al* [38] have recently proposed that electron parallel transport will cause flattening for much thinner islands than sound waves. The characteristic island width $W_\parallel$ above which parallel transport dominates diamagnetic drifts is determined by $\omega_{*e} = k_\parallel^2 D_\parallel$, where $D_\parallel = T_e / 0.51 m_e \nu_e$ and ν_e is the electron collision frequency. This leads to $W_\parallel = \rho_s C^{1/2}$, where $C = 0.51(\nu_e/\omega_{*e})(m_e/m_i)(L_s/L_n)^2$ is a measure of collisionality introduced by Drake *et al* [19]. In the semi-collisional regime of interest to fusion experiments, $C \ll 1$ so that $W_\parallel \ll W_a$. The characteristic width $W_\parallel$ is identical to the width of the current channel for linear drift-tearing modes, so that the parallel transport is a dominant effect as soon as the island enters the quasilinear regime, for $W \sim W_\parallel \sim \rho_s C^{1/2}$.

Unfortunately, the numerical literature provides disparate answers for the natural propagation velocity and fails to resolve the question of whether W_a or $W_\parallel$ best describes the characteristic width for flattening. Biskamp [39] and Hicks *et al* [40] have presented evidence for flattening caused by parallel transport. Monticello and White [41], however, have reported that they found no flattening when the island was initiated in the nonlinear regime with a width such that $W_\parallel \ll W \ll W_a$. Scott *et al* [42] did not specify the velocities of the islands they studied (except in the quasilinear regime), but their observation of sustained growth for islands seeded above the quasilinear threshold are consistent with the results of Monticello and White. Ottaviani *et al* [38] found bifurcations between large islands with flattened density and small islands with unflattened density profiles. Recently, Fitzpatrick *et al* carried out two extensive numerical studies [36,43]. In the first, they used a model with finite ion temperature and electron viscosity and found that islands with $W \leqslant W_a$ had flattened density and that their phase velocity was reduced from the diamagnetic velocity. In the second study, they used a constant-$\tilde{\psi}$ approximation to scan the entire range of W/ρ_s values from $W \ll \rho_s$ to $W \gg W_a$. They confirmed the existence of a bifurcation for $W/\rho_s \sim 1$ between a state with no flattening and a state with moderate flattening, which they identified as an electron and an ion branch, respectively. We will discuss the numerical results further in the conclusion to the present paper and propose an explanation for some of the apparent discrepancies in the literature.

The experimental data, in contrast to the simulations, consistently indicate that flattening occurs for $W \sim W_a$, corresponding to acoustic flattening [12,13,44]. The observations are less conclusive, however, when it comes to the phase velocity of magnetic islands. This is because the electric drift dominates the diamagnetic drift in tokamaks, making it difficult to determine the island velocity in the plasma frame. In Ohmic discharges, it has generally been concluded that islands propagate in the electron diamagnetic direction [45–48]. In a recent study of

DIII-D beam-heated plasmas, however, Lahaye *et al* came to the opposite conclusion that the phase velocity is close to the ion drift velocity in discharges with unbalanced momentum injection [49].

In the present paper, we neglect the ion temperature for simplicity and restrict attention to the regime defined by $W_\parallel \ll W \ll \rho_s$. The lower limit ensures that the transport ordering is satisfied, in the sense that the parallel and perpendicular transport rates are respectively fast and slow compared with dynamical processes such as the electric and diamagnetic drifts. The upper limit defines what we will refer to as the *unmagnetized island* regime, although we note that the island is magnetized in the conventional sense since the ion gyroradius is zero in our model. Coupling to the sound wave can be neglected in the unmagnetized regime provided that $L_n < L_s$, so that the parallel velocity can be neglected: the plasma flows are non-compressive. In a companion paper we will describe the magnetized non-compressive island regime $\rho_s \ll W \ll W_a$. The compressive regime, $W_a \ll W$, has been described in [34–36]. We note that in these references the compressive and non-compressive regimes are denoted as subsonic and supersonic, based on the ordering of $\omega/k_\parallel$ with respect to c_s. In both regimes our ordering retains the parallel transport effects pointed out in [38]. We determine the phase velocity by solving a system of coupled equilibrium and transport equations derived previously by Connor *et al* [28] and use the results to determine the effect of the polarization current. A condensed account of some of the results of the present work can be found in [50].

The paper is organized as follows. In section 2 we summarize the equations used. We describe the numerical solutions of the nonlinear equations in section 3. We next briefly review the linear solution in section 4.1 in order to set the context for the presentation in section 4.2 of the analytic solution of the nonlinear problem in the unmagnetized limit ($W \ll \rho_s$). We discuss our results and conclude in section 5.

2. Formulation

2.1. The drift model

We consider a two-fluid, cold-ion model consisting of Ohm's law and the vorticity, electron continuity and heat equations, respectively:

$$D_t\psi + \nabla_\parallel n + \hat{\alpha}\nabla_\parallel T = Cj, \tag{1}$$

$$D_t U - \nabla_\parallel j_\parallel = \mu\nabla_\perp^2 U, \tag{2}$$

$$D_t n - \nabla_\parallel j = D\nabla_\perp^2 n, \tag{3}$$

$$D_t T - \tfrac{2}{3}\hat{\alpha}\nabla_\parallel j = \kappa_\parallel\nabla_\parallel^2 T + \kappa_\perp\nabla_\perp^2 T. \tag{4}$$

We have normalized the time to $-1/\omega_{*e}$, the transverse distances to ρ_s ($x = X/\rho_s$) and the azimuthal distances to k_Y^{-1} ($y = k_Y Y$). The electrostatic potential is normalized so that the adiabatic response is $n = \varphi$. $U = \nabla_\perp^2\varphi$ describes the vorticity, and

$$j = (\nabla^2\psi - 1)/\hat{\beta} \tag{5}$$

is the current where ψ is the flux normalized to $B_0\rho_s^2/L_s$. The '-1' term in (5) corresponds to the background inductive electric field. The operator $D_t = \partial_t + \boldsymbol{v}_E\cdot\nabla$, where $\boldsymbol{v}_E = \hat{\boldsymbol{z}}\times\nabla\varphi$ represents the convective derivative along the $\boldsymbol{E}\times\boldsymbol{B}$ flow, $\nabla_\parallel = \hat{\boldsymbol{z}}\cdot\nabla\psi\times\nabla$ represents the derivative in the direction of the magnetic field and $\partial_t = \partial/\partial t$. Lastly, the terms on the right-hand sides of the equations represent transport phenomena described by the radial (ambipolar) diffusion coefficient D, the viscosity μ, the perpendicular heat conductivity $\kappa_\perp$, the parallel heat conductivity $\kappa_\parallel = \hat{\kappa}/C$ and the normalized resistivity $C = 0.51(\nu_e/\omega_{*e})(m_e/m_i)(L_s/L_n)^2$.

The remaining symbols $\hat{\alpha}$ and $\hat{\kappa}$ are numerical constants that take the values $\hat{\alpha} = 1.71$ and $\hat{\kappa} = 1.09$ in the case of classical transport.

We are interested in steady-state solutions of equations (1)–(4) representing saturated magnetic islands propagating at constant velocity. We consider thin islands such that $w = k_y W \ll 1$, so that $\nabla^2 \simeq \partial_x^2$. It is convenient to work in a frame where the island is at rest, so that $\partial_t = 0$. For simplicity, we restrict our attention to states such that ψ is an even function of x while n, φ and T are all odd functions of x. We will write the results for $x > 0$ only. The symmetry assumption implies that on the midplane $\partial_x \psi(0, y) = 0$ and $n(0, y) = \varphi(0, y) = T(0, y) = 0$.

The boundary conditions at large distances from the island are as follows. For the density and temperature, we require that $n \sim x$ and $T \sim \eta_e x$ at large x. The electron diamagnetic velocity in the reference state is thus $\boldsymbol{v}_D = -(1 + \eta_e)\hat{\boldsymbol{y}}$. The magnetic flux must match the linear solution away from the island,

$$\psi \sim \frac{x^2}{2} + \left(1 + \frac{\Delta' \rho_s}{2} |x|\right) \tilde{\psi} \cos y, \tag{6}$$

where $\tilde{\psi}$ is the perturbation amplitude and Δ' is the conventional measure of the external drive for the tearing mode.

Regarding the electrostatic potential, we wish to choose a boundary condition such that the external electromagnetic forces acting on the island vanish. In the absence of volumetric momentum sources, such as neutral beams, the force balance requires that the momentum flux vanish away from the island,

$$\lim_{x \to \infty} \mu \bar{v}_y' = 0, \tag{7}$$

where the overbar denotes an average over y. Since equation (2) is fourth order and we have assumed that φ is odd, we must specify a second boundary condition at ∞. It follows from equation (7) that

$$\lim_{x \to \infty} \bar{v}_y = v_\infty, \tag{8}$$

where v_∞ is a constant. If the value of v_∞ were known, we could adopt equation (8) as our second boundary condition. Since this value is unknown, however, we are driven to solve as an intermediate step the problem corresponding to the following more general boundary conditions:

$$v_y(x_{\text{edge}}, y) = v_{\text{edge}}(y), \tag{9}$$

$$v_y''(x_{\text{edge}}, y) = 0, \tag{10}$$

where the y-dependence of v_{edge} is chosen such as to be compatible with a frozen-in flow, $v_{\text{edge}}(y) = \bar{v}_{\text{edge}} B_y(x_{\text{edge}}, y)/\bar{B}_y(x_{\text{edge}})$. The first of these boundary conditions represents a no-slip boundary condition on a wall moving at velocity $\bar{v}_{\text{edge}}$ in the frame where the island is at rest. The second boundary condition indicates the absence of a volumetric momentum source. From the solution of this problem one obtains the viscous force as a function of $\bar{v}_{\text{edge}}$, $F_y(\bar{v}_{\text{edge}}) = \mu v_y'(x_{\text{edge}})$. The edge velocity $\bar{v}_{\text{edge}}^{\text{free}}$ corresponding to force-free propagation is then determined by $F_y(\bar{v}_{\text{edge}}^{\text{free}}) = 0$.

By convention, the natural frequency ω of the island is measured in the frame where the electric drift vanishes away from the island. The natural frequency of the island is thus related to the velocity $\bar{v}_{\text{edge}}^{\text{free}}$ of the plasma in the island frame by

$$\omega = -\bar{v}_{\text{edge}}^{\text{free}}, \tag{11}$$

where the overbar denotes averaging over y. The minus sign is familiar to anyone who has ever observed the landscape moving backwards from a train.

We may reduce the number of control parameters by making use of appropriate orderings. First we restrict our attention to the weak collisionality regime, such that the transport coefficients are small: C, μ, D and $\kappa_\perp \ll 1$. With this ordering the solutions depend only on the three ratios of transport parameters $Sc = \mu/D$, $Le = \kappa_\perp/D$ and $Fz = (\kappa_\parallel\kappa_\perp)^{1/4}$ (note that all transport coefficients are dimensionless with our normalizations). The Schmidt number $Sc = \mu/D$ is most commonly used to describe the diffusion of passive scalar fields in a turbulent fluid, while the Lewis number $Le = \kappa_\perp/D$ is most often used to describe the propagation of flame fronts. We have introduced the parameter Fz to describe the ratio between the characteristic width for the flattening of the temperature profile and the linear layer width, $C^{1/2}$. We will refer to this as the Fitzpatrick number [51]. In this paper we will assume that temperature profiles are flattened or that $C^{1/2}Fz \ll W/\rho_s \ll 1$.

In the following subsection, section 2.2, we present the IslET model obtained by using this ordering to reduce the system (1)–(4) to a set of equilibrium and transport equations in the steady-state limit. In the subsequent section, section 2.3, we further simplify the equilibrium and transport equations by using the constant-$\tilde{\psi}$ approximation. As can be seen from equation (5), $\nabla^2\psi = 1 + O(\hat{\beta})$ so that the constant-$\tilde{\psi}$ approximation is justified whenever $\hat{\beta} \ll 1$ and $\Delta' w \ll 1$. With the above approximations, the solution is determined by the single equilibrium parameter $\hat{\Delta}'$ as well as the three ratios of transport coefficients that control the profiles near the island.

2.2. *Equilibrium and transport*

In the steady-state case, all the time derivatives vanish in the frame where the island is at rest. In this case the smallness of the transport coefficients can be used to partly solve the governing equations (1)–(4) and reduce them to a set of 1.5-dimensional equations. We will call the reduced 1.5D model the island equilibrium and transport (IslET) model. Reference [28] contains a detailed derivation of the IslET model.

In the IslET model all the physical quantities are determined in terms of the two basic fields φ and ψ and two profile functions that are related to the isothermal electron streamfunction $H(\psi) = n - \varphi$ (the complete electron stream function is $H + T$) and a function $K(\varphi)$ related to the potential vorticity.

The magnetic flux is determined by the two-fluid Grad–Shafranov equation,

$$\nabla^2\psi = 1 - \hat{\beta}H'(\psi)\tilde{\varphi}, \tag{12}$$

where

$$\tilde{\varphi} = \varphi - \frac{\langle\varphi\rangle_\psi}{\langle 1\rangle_\psi}.$$

The second term in equation (12) represents the polarization current. The electrostatic potential is determined by

$$\nabla^2\varphi = K(\varphi) + H(\psi). \tag{13}$$

The above two equations are consequences of force balance. The profile functions K and H, by contrast, are determined by transport processes. For the cold-electron stream function we have

$$\frac{\mathrm{d}H}{\mathrm{d}\psi} = \frac{\left(1 - \langle\partial^\psi\varphi\rangle_\psi\right)\Gamma + \hat{\alpha}\,\eta_e\,Fz^{-4}\,Le\,\Upsilon}{\langle x^2\rangle_\psi\Gamma + Fz^{-4}\,Le\,\Upsilon\left(\hat{\kappa}\Gamma + \frac{2}{3}\hat{\alpha}^2\langle x^2\rangle_\psi\right)}, \tag{14}$$

where

$$\Upsilon = \langle \tilde{\varphi}^2 \rangle_\psi = \langle \varphi^2 \rangle_\psi - \langle \varphi \rangle_\psi^2 / \langle 1 \rangle_\psi$$

and $\Gamma = \langle x^2 \rangle_\psi + F z^{-4} \Upsilon$. Here $\partial^\psi \varphi = \nabla\psi \cdot \nabla\varphi$ is the contravariant ψ-derivative of φ and the angular brackets $\langle \cdot \rangle_\psi$ represent the integral over a surface of constant flux,

$$\langle f \rangle_\psi = \begin{cases} \oint \dfrac{\mathrm{d}y}{|\psi_x|} f(x, y), & \psi > \psi_\mathrm{s}, \\ \displaystyle\int_{-y_t}^{y_t} \frac{\mathrm{d}y}{2|\psi_x|} [f(x, y) + f(-x, y)], & \psi < \psi_\mathrm{s}, \end{cases}$$

where ψ_s is the value of the flux on the separatrix, $\pm y_t(\psi)$ are the turning points for flux surfaces inside the separatrix and $\psi_x = \partial\psi/\partial x$. Lastly, the profile K determining the potential vorticity is given by

$$\frac{\mathrm{d}K}{\mathrm{d}\varphi} = \frac{1}{Sc}\left(1 - \frac{1}{\langle \varphi_x^2 \rangle_\varphi}\right) + \left(\frac{1}{Sc} - 1\right) \frac{\langle \varphi_x \partial_x H(\psi) \rangle_\varphi}{\langle \varphi_x^2 \rangle_\varphi}, \tag{15}$$

where the average $\langle \cdot \rangle_\varphi$ is a streamline average defined in a way analogous to the flux-surface average.

Equations (12)–(15), completed by the boundary conditions (6) and (9)–(10), constitute the complete nonlinear IslET model that determines the size and velocity of magnetic islands. The remaining quantities are given in terms of the basic fields by

$$\begin{aligned} n &= \varphi + H(\psi), \\ j &= -H'(\psi)(\varphi - \langle \varphi \rangle_\psi / \langle 1 \rangle_\psi), \end{aligned} \tag{16}$$

$$T = \frac{\eta_\mathrm{e} + \frac{2}{3}\hat{\alpha} F z^{-4} \Upsilon H'}{\langle x^2 \rangle_\psi + F z^{-4} \Upsilon}. \tag{17}$$

In view of the reduced nature of the IslET model compared with the complete dynamical model, it is necessary to revisit the question of boundary conditions. The parity we have assumed determines the boundary conditions for the two profile functions, $K(0) = 0$ and $H(\psi) = 0$ for $\psi < \psi_\mathrm{s}$. It also specifies one boundary condition for the equilibrium equation (13), namely, $\varphi(0, y) = 0$ for all y. For the second boundary condition on φ, we recall that the change in the vorticity across the island region is proportional to the total viscous force F_y acting on the island:

$$\bar{U}(x_\mathrm{edge}) \simeq \bar{v}_y'(x_\mathrm{edge}) = F_y/\mu. \tag{18}$$

In the absence of an opposing electromagnetic force, F_y must vanish. It is tempting, in order to calculate the force-free solutions directly, to require $U(x_\mathrm{edge}, y) = 0$ *for all* y. Unfortunately, this over-determines the solution and leads to a boundary layer of width ρ_s at the edge. To see this, consider the asymptotic solution of the equilibrium equation for large x. To lowest order in $1/x$ one finds $\varphi = \varphi_0 = K^{-1}(-H(\psi))$. The corresponding vorticity does not satisfy the boundary condition $U \simeq \partial_x^2 \varphi = 0$, however, so it is necessary to add a small correction $\varphi = \varphi_0 + \varphi_\mathrm{hom}$, where φ_hom is a solution of the homogeneous equation

$$\partial_x^2 \varphi - K'(\varphi_0)\varphi = 0.$$

This small correction varies on the scale $1/\sqrt{K'} \ll x_\mathrm{edge}$. This is the boundary layer referred to above. The point is that only $\bar{U}(x_\mathrm{edge}) = 0$ is needed, rather than the stronger condition $U(x_\mathrm{edge}, y) = 0$ for all y.

We settle the question of boundary conditions by specifying the edge velocity according to equation (9). The resulting solutions describe the two cases where either the flow is being

forced around the island or the island is being dragged through the plasma. The first case arises when plasma flows are driven by a source of momentum such as neutral beams while the island is locked to static external structures. The second case arises when the island is locked to phased AC error fields that generate a travelling wave. Such fields are sometimes applied for control purposes.

In the present paper, however, we are primarily interested in the case of free propagation. We thus determine the corresponding solution by varying the edge velocity $v_{\rm edge}^{\rm free}$ so as to satisfy the condition $\bar{U}(x_{\rm edge}) = 0$. The natural frequency ω is then given by equation (11).

2.3. Constant-ψ regime

For small $\hat{\beta}$, the variation of the amplitude of the flux perturbation may be neglected in the island region and the flux may be approximated by

$$\psi = \tfrac{1}{2}[x^2 + w^2 \sin^2(y/2)],$$

where $w = W/\rho_{\rm s} = (4\tilde{\psi} L_{\rm s}/B_0)^{1/2}/\rho_{\rm s}$ is the normalized half-width of the island. The normalized half-width w is determined implicitly by the boundary condition

$$\hat{\Delta}'(w) + \hat{\Delta}_{\rm pol}(w) = 0, \tag{19}$$

where $\hat{\Delta}'(w) = \Delta'(w)\rho_{\rm s}/\hat{\beta}$ is the normalized measure of the drive for the tearing mode [52,53] and

$$\hat{\Delta}_{\rm pol}(w) = \frac{16}{w^2}\int_0^\infty {\rm d}\psi\ \langle j \cos y\rangle_\psi \tag{20}$$

is the normalized integral of the polarization current. Recall that aside from the ratios of the transport coefficients, $\hat{\Delta}'$ is the *only* free dimensionless parameter in the constant-$\tilde{\psi}$ approximation.

The constant-$\tilde{\psi}$ approximation allows us to omit equation (12) from the IslET model and to solve the system of equations (13)–(15) only. We describe the numerical and analytic solutions of these equations in the following two sections.

3. Numerical solution

We solve the constant-$\tilde{\psi}$ IslET equations numerically using a generalized Picard iteration procedure. The procedure makes use of the fact that the equilibrium equation (13) determines φ in terms of the profile functions K and H only, while the transport equations (14) and (15) determine K and H in terms of the electrostatic potential φ only. The algorithm thus consists of making an initial guess for the profile functions K and H and then solving the equilibrium and the transport equations successively until the solution converges.

Figure 2 shows the average along the stream lines of the azimuthal velocity, $\bar{v}_y = \oint \partial_x\varphi\, {\rm d}y/2\pi = \langle \partial^\varphi \varphi\rangle_\varphi$, for a scan of the edge velocity with $w = 0.5$, $Sc = Le = 1$, $Fz = 0.84$ and $\eta_{\rm e} = 1.0$. The solution corresponding to free propagation, $v'_\infty = 0$, is indicated by a thick line. For the parameters used in figure 2 the natural velocity is $\omega \simeq -0.8$. The results show that in the general case where the flow is forced, the average of the central velocity deviates from the central natural velocity by a fraction of the difference between the edge velocity and the edge natural velocity,

$$\langle v_y\rangle(0) - v_{\rm free}(0) \simeq \lambda(v(x_{\rm edge}) - v_{\rm free}(x_{\rm edge})),$$

where the coefficient $\lambda(w)$ decreases with increasing w. The difference between the edge and natural velocities is proportional to the gradient of the velocity away from the island and thus

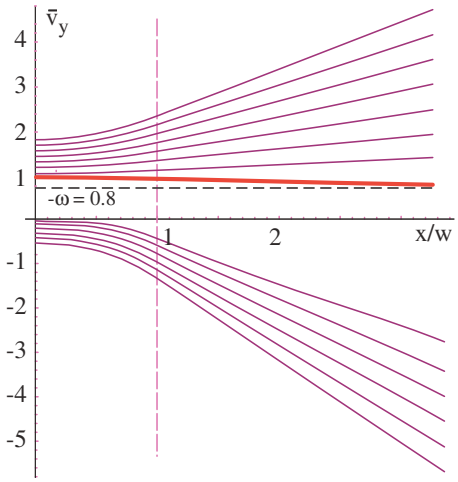

Figure 2. Average along the stream lines of the azimuthal plasma velocity, $\bar{v}_y$, for various values of the applied force. The parameters are $\eta_e = 1.0$, $Sc = Le = 1.0$ and $Fz = 0.84$ resulting in $\omega = -0.8$. The thick line is the profile corresponding to free propagation and the dashed vertical line indicates the width of the island.

to the viscous force acting on the island. The coefficient λ is thus inversely proportional to the drag coefficient. Note that since the total electron velocity must vanish inside the separatrix, any variation in the electric drift inside the separatrix must be compensated by a corresponding change in the local diamagnetic drift. It follows that driving the flow in the direction of the electron drift velocity results in a *steepening* of the density profile inside the island, whereas driving the flow in the ion direction results in flattening and, for sufficiently strong drive, reversing the density gradient.

The gap in figure 2 in the range $0 < v(0) < v_{\text{free}}(0)$ corresponds to cases where the plasma velocity changes sign between the midplane and the edge ($v(0) > 0$ but $v'_\infty < 0$). In such cases convergence fails. The loss of convergence appears to be related to the formation of convection cells in the presence of velocity reversal. The domain of non-convergence, however, extends significantly beyond the region of parameters where we expect convection cells, so that stability is the primary limitation of the code.

The reason for expecting convection cells in the presence of velocity reversal is the following. The vanishing of the velocity, $\partial\varphi/\partial x = 0$, indicates the presence of a maximum of φ along a chord of constant y. The value of the maximum generally varies from chord to chord so that there will be an absolute maximum at some value of y, $\varphi_{\max} = \max_y(\max_x(\varphi(x, y))$. Such a maximum in φ constitutes the O-point of a convection cell. In cases where $v_{\text{free}}(\text{O-point}) > 0$, we may expect the velocity to change sign when the island is being driven in the ion direction with insufficient force to cause $v_y(\text{O-point}) < 0$. When the island is being driven in the electron direction, by contrast, the velocity remains positive definite. We note that solutions of the equilibrium equation that use a linear ansatz for $K(\varphi)$ [29] also predict the presence of convection cells for velocities intermediate between the guiding centre velocity and the electron diamagnetic drift velocities. Such convection cells are associated with the excitation of drift-acoustic waves by the island [29, 54].

The first two coefficients in the asymptotic form of the velocity at large x,

$$\bar{v}_y(x) = v'_\infty x + \delta v_\infty + O(1/x), \tag{21}$$

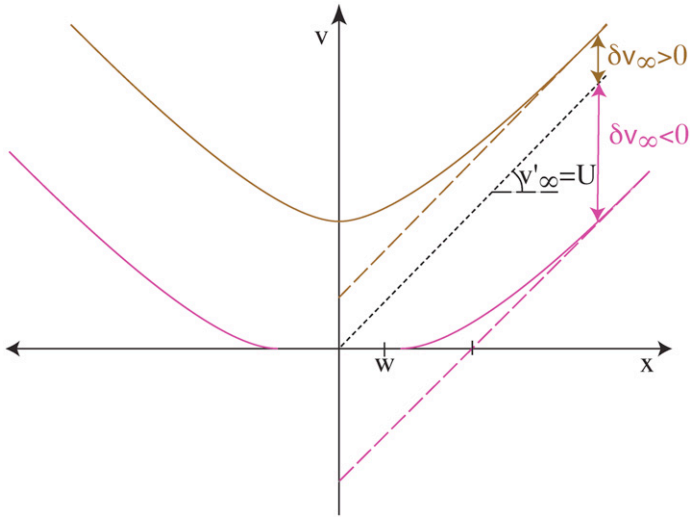

Figure 3. Sketch of two velocity profiles illustrating the concept of island permeability and its parametrization in terms of the asymptotic slip velocity δv_∞. The upper and lower curves represent a typical profile in a permeable and an impermeable island, respectively.

provide the information needed in order to match the solutions away from the island to the solutions in the remainder of the plasma where effects that are neglected in the present paper, such as geometrical effects and the spatial variation of the transport coefficients, may be important. The gradient v'_∞ is proportional to the viscous force acting on the island. The asymptotic shift in the velocity δv_∞, by contrast, measures the degree of permeability of the island to the plasma flow, as illustrated in figure 3. The dotted line in this figure shows a V-shaped profile such as would result from inserting a thin plate with a no-slip boundary condition in the middle of the plasma. The top curve shows a velocity profile for a permeable island where the plasma flows relatively easily through the island, so that the entire velocity profile is shifted upwards compared with the no-slip V-profile. The bottom curve, by contrast, shows the opposite limit of a highly impermeable island where the flow is excluded from within the separatrix. In this case the velocity profile at a large distance is shifted downwards from the no-slip profile.

Figure 4 shows the variation of the slip velocity, δv_∞, and of the integral of the polarization current, $\hat{\Delta}_{\rm pol}$, as a function v'_∞ (which is proportional to the force) for various islands sizes. We will refer to the first set of curves as the slip curves and to the second as the polarization curves. The slip curves show that unmagnetized islands ($w \ll 1$) are permeable, in the sense that δv_∞ is positive and approximately equal to the velocity of the plasma flow through the separatrix. Magnetized islands ($1 \ll w \ll L_s/L_n$), by contrast, are highly impermeable as shown in [50]. In magnetized islands the velocity is held very close to the natural frequency everywhere inside the separatrix, leading to $\delta v_\infty \simeq \bar{v}_{\rm free}(0) - v'_\infty w$.

The propagation velocity of the island in the plasma frame is given by the negative of the intersection of the slip curves with the ordinate. For the parameters of figure 4 $\omega = -0.8$. For most values of the applied force we see that $\delta v_\infty > 1$ resulting in a destabilizing effect of the polarization current, $\Delta_{\rm pol} > 0$ [28]. For $v'_\infty < 0.6$, however, and in particular for the natural propagation solution corresponding to $v'_\infty = 0$, the polarization integral is negative, showing a stabilizing polarization current.

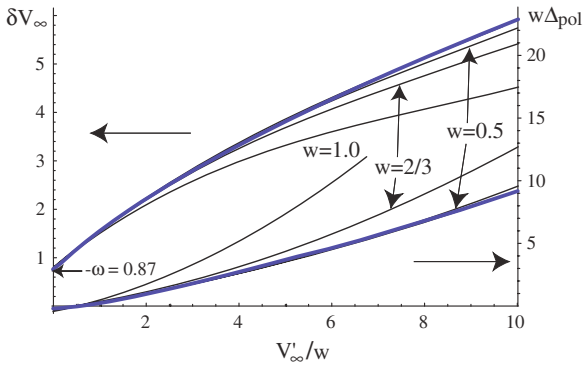

Figure 4. Slip velocity δv_∞ (top curves) and stability parameter $\Delta_{\rm pol}$ (scaled to the inverse island width, bottom curves) for unmagnetized islands ($w = W/\rho_{\rm s} \leqslant 1$) as a function of the forcing at the boundary scaled to the island width. The natural velocity, given by the intercept of the slip curves with the ordinate, is approximately 0.8 for these parameters. The thick lines at the top and bottom represent the analytic asymptotic results for $w \ll 1$ given by equations (32)–(34) and (35)–(37). The positive slope of the slip curves for $w \leqslant 1$ shows the permeable nature of unmagnetized islands. The parameters are $Fz = Sc = 1$, $Le = 1.7$ and $\eta_{\rm e} = 1$.

We note that we have not investigated the stability of the roots with respect to changes in the propagation velocity. It is possible that an instability of the phase velocity would manifest itself as an instability in the IslET code, but the algorithm used in the code is distinct from the actual temporal evolution equations so that numerical and physical stabilities are unrelated.

In order to better understand the numerical results and to obtain solutions in regions where the IslET code fails to converge, we next describe analytic solutions of the IslET equations in the unmagnetized island regime. Analytic solutions for the magnetized non-compressive ($\rho_{\rm s} \ll W \ll \rho_{\rm s} L_{\rm s}/L_n$) and compressive ($\rho_{\rm s} L_{\rm s}/L_n \ll W$) regimes for $\eta_{\rm e} = 0$ can be found in [50] and [34–36], respectively.

4. Analytic solution

4.1. Linear regime

It is instructive to briefly review the results of the linear theory [19]. For $D = \mu = 0$, the consequences of drifts and of the electron thermal motion can be described entirely in terms of the effects of a spatially varying conductivity $\sigma(x)$. That is, the mode equations take the same form as in MHD,

$$\tilde{\varphi}'' = {\rm i}x(\tilde{\psi} + x\tilde{\varphi}/\omega)\sigma(x), \tag{22}$$

$$\tilde{j} \;\; = \; -{\rm i}\omega(\tilde{\psi} + x\tilde{\varphi}/\omega)\sigma(x), \tag{23}$$

except that the conductivity now depends on x through $\sigma(x) = \hat{\sigma}({\rm i}x^2/C\omega)$ where

$$\hat{\sigma}(s) = -\frac{1}{C\omega}\,\frac{(\omega+1)(1+\hat{\kappa}s) + \hat{\alpha}\eta_{\rm e}}{1 + (1 + \hat{\kappa} + \frac{2}{3}\hat{\alpha}^2)s + \hat{\kappa}s^2}. \tag{24}$$

For $\hat{\beta} \ll 1$ the above equations may be solved by using the constant-$\tilde{\psi}$ approximation. Inspection of the conductivity shows that it falls rapidly outside a channel of width $\Delta_D = (-C\omega)^{1/2} \ll 1$ reflecting the screening of the electric field by the parallel thermal motion of the electrons. The electrostatic field, however, varies on the much larger scale $\rho = 1/\sqrt{1 + 1/\omega}$,

as can be seen from equation (22). Although the contribution of the electrostatic field to the current density is small compared with that due to the induction, its greater spatial extent means that it must be taken into account. In the region $\Delta_D \ll x \sim \rho$, the vorticity equation (22) simplifies to

$$\rho^2\varphi''(x) - \varphi(x) = \omega\tilde{\psi}/x. \tag{25}$$

The solution is $\tilde{\varphi}(x) = -(\omega\tilde{\psi}/\rho)\hat{\varphi}(x/\rho)$, where

$$\hat{\varphi}(z) = \tfrac{1}{2}[\mathrm{e}^{-z}\,\mathrm{Ei}(z) + \mathrm{e}^{z}\,\mathrm{E}_1(z)]$$

and $\mathrm{Ei}(z)$ and $E_1(z)$ are the standard exponential integrals [42]. The dispersion relation is evaluated in a straightforward way by substituting the current from Ohm's law, equation (23), into the matching relation (19). There follows

$$\hat{\Delta}' = 1.4\mathrm{e}^{-3\mathrm{i}\pi/4}\omega(\omega - \omega_1)\Delta_D^{-1} + \frac{\pi^2}{2}\omega(\omega+1)\rho^{-1}, \tag{26}$$

where

$$\omega_1 = -1 - \hat{\alpha}\eta_\mathrm{e}/(1+\hat{\kappa}^{1/2}). \tag{27}$$

The first term in the dispersion relation (26) corresponds to the current flowing in the conduction channel of width Δ_D and the second to the polarization current flowing in the inertial layer of width ρ.

For sufficiently large drive, $C^{-1/2} \ll \hat{\Delta}'$, the first term dominates and the mode is purely growing with $\omega = \mathrm{i}(\hat{\Delta}'/1.4)^{2/3}C^{1/3}$. In order for the channel width to remain less than 1 (the inertial layer width) the driving term must also satisfy $\hat{\Delta}' \ll C^{-2}$. In the corresponding regime, $1 \ll C^{-1/2} \ll \hat{\Delta}' \ll C^{-2}$ the mode is called a semi-collisional tearing mode. For weaker drive, $\hat{\Delta}' \ll C^{-1/2}$, the growth rate becomes comparable to the real part of the frequency and the instability becomes a drift-tearing mode. The contribution of the conduction channel dominates and to lowest order the dispersion relation requires that $\omega = \omega_1 + O(C^{1/2}) \gg \gamma$, whence $\Delta_D \sim C^{1/2}$. The growth rate is then determined by the balance between the drive term proportional to $\hat{\Delta}'$ and the polarization term. Complete stabilization results when

$$\hat{\Delta}' < f(\eta_\mathrm{e}) \equiv \pi^2[\omega_1(\omega_1+1)^3]^{1/2}/2. \tag{28}$$

Scott *et al* [42] have shown that quasilinear effects lead to the saturation and decay of the linear drift-tearing mode, but that islands initially wider than the current channel experience continued growth [42]. We next consider the nonlinear theory for such islands.

4.2. Thin-island regime: outer region solution

When the island width exceeds the width of the conduction channel it replaces the latter as the scale of the thinnest current structure. To obtain a complete solution it is necessary to separate the problem into the island region, $x \sim w \ll 1$, and the outer region $x \sim 1 \gg w$. We first consider the solution in the outer region.

In this region, we may solve the equilibrium equation by expanding the H function in a Taylor series:

$$\partial_x^2\varphi = K(\varphi) + H(x^2/2) + H'(x^2/2)\frac{w^2}{2}\sin^2\frac{y}{2} + O(w^4).$$

This shows that φ takes the form

$$\varphi(x,y) = \Phi_0(x) + w^2\Phi_1(x)\sin^2 y/2 + O(w^4).$$

Note that φ is a function of x alone at lowest order.

To specify the precise form of Φ_0 we must first determine K and H. We substitute Φ_0 in the transport equations (14) and (15) and note that $\langle(\partial_x\varphi)^2\rangle_\varphi \to d\Phi_0/dx$ and $\Upsilon \to 0$. After integrating the transport equations there follows

$$H_0(\psi) = \sqrt{2\psi} - \Phi_0(\sqrt{2\psi}) + \delta H_\infty$$

and

$$K_0(\varphi) = \frac{1}{Sc}\left(\varphi - \Phi_0^{-1}(\varphi)\right) + \left(\frac{1}{Sc} - 1\right) H_0\left[(\Phi_0^{-1}(\varphi))^2/2\right] + \delta K_\infty,$$

where δH_∞ and δK_∞ are integration constants that must be determined by matching the solution to that found in the inner region. To lowest order, the equilibrium equation is thus

$$\partial_x^2\Phi_0(x) = U_\infty,$$

where v_0 is the electric drift velocity in the island region and $U_\infty = \delta K_\infty + \delta H_\infty/Sc$ is the constant velocity shear. The solution is

$$\Phi_0 = (U_\infty|x|/2 + v_0)x.$$

This completes the determination of the lowest-order solution aside from the two parameters δH_∞ and δK_∞, which are determined by matching to the inner solution. Substituting our results into the polarization current, equation (16), however, we see that the outer region does not contribute to the lowest-order j or to the matching integral, equation (19), since $\varphi = \langle\varphi\rangle_\psi/\langle 1\rangle_\psi + O(w^2)$. For this reason it is of interest to evaluate the first-order corrections in the outer region.

Omitting corrections depending on x alone (these can be incorporated into Φ_0), the first-order equilibrium equation takes the form

$$\Phi_1''(x) = K_0'(x)\Phi_1 + \tfrac{1}{2}H_0'(x^2/2).$$

Substituting the form of K_0 and H_0 found above and restricting consideration to the case $U_\infty = 0$, the equilibrium equation becomes

$$(1 - 1/v_0)^{-1}\Phi_1''(x) - \Phi_1 = -\frac{v_0}{x}.$$

We recognize the equation found in the linear theory, equation (25), for the electrostatic potential in the inertial (outer) region, with $v_0 = -\omega$. This is as expected: away from the island linear theory should apply. The solution is $\Phi_1(x) = (v_0/\rho)\hat{\varphi}(x/\rho)$, where $\hat{\varphi}$ is defined in the previous subsection. The contribution of the outer region to the polarization integral is thus identical to that for the linear regime.

4.3. Thin-island regime: inner region solution

In the island region, $x \sim w \ll 1$, we may solve the equilibrium equation by observing that $\nabla^2 \sim w^{-2} \gg 1$, so that to lowest order equation (13) reduces to Laplace's equation, $\nabla^2\varphi_0 = 0$. The solution is

$$\varphi = v_0 x + O(w^2),$$

where v_0 is the electric drift velocity in the island frame (i.e. v_0 is the negative of the propagation velocity in the frame where the electric drift vanishes). Substituting the lowest-order solution $\varphi_0 = v_0 x$ in the transport equations (14) and (15), we may evaluate $\mathrm{d}K/\mathrm{d}\varphi$ and $\mathrm{d}H/\mathrm{d}\psi$ in terms of v_0. Note that using the lowest-order solution in this fashion is a 'constant-v' approximation, analogous to the well-known constant-$\tilde{\psi}$ approximation. Both approximations fail when the lowest-order term is small. In the present case, we see that higher-order corrections become important when $v_0 = O(w)$.

We begin by evaluating the stream average of $\partial^\varphi H$ that appears in the equation for $dK/d\varphi$,

$$\langle \partial^\varphi H(\psi)\rangle_\varphi = \oint \frac{\mathrm{d}y}{2\pi}\, x \frac{\mathrm{d}H}{\mathrm{d}\psi},$$

where the integral is to be carried out at constant φ or equivalently at constant x. Substituting this in equation (15) and integrating with respect to $\varphi_0 = v_0 x$, we find

$$K(\varphi) = \frac{1}{Sc}\left(1-\frac{1}{v_0}\right)\varphi + \left(\frac{1}{Sc}-1\right)\oint \frac{\mathrm{d}y}{2\pi}\, H\left[\frac{1}{2}\left(\frac{\varphi}{v_0}\right)^2 + \frac{w^2}{2}\sin^2\frac{y}{2}\right].$$

The asymptotic form of K for $w \ll x \ll 1$, or for $wv_0 \ll \varphi \ll v_0$, is

$$K(\varphi) \sim \frac{1}{Sc}\left(1-\frac{1}{v_0}\right)\varphi + \left(\frac{1}{Sc}-1\right) H\left[\frac{1}{2}\left(\frac{\varphi}{v_0}\right)^2\right] + O\left(\frac{w^2 v_0^2}{\varphi^2}\right).$$

Matching this expression to that for K in the outer region shows that $\delta K_\infty = 0$.

We next calculate the asymptotic form of the vorticity $U = \nabla^2\varphi$ using the equilibrium equation:

$$U = K(\varphi) + H(\psi) \sim Sc^{-1}[(v_0-1)x + H(x^2/2) + O(w^2/x^2)].$$

We see that the vorticity is inversely proportional to the Schmidt number.

The asymptotic form of $H(\psi)$ is complicated due to the numerous terms in equation (14). For the sake of clarity we begin by presenting the limit $Le \ll 1$.

4.3.1. Limit of the small Lewis number. In this limit the equation for H simplifies considerably. We may evaluate the only remaining geometric factor by using $\varphi = v_0 x$, whence it is easy to see that $\langle \partial^\psi \varphi\rangle_\psi = v_0$. The equation for H thus reduces to

$$\frac{\mathrm{d}H}{\mathrm{d}\psi} = \frac{1-v_0}{\langle x^2\rangle_\psi}. \tag{29}$$

Substituting the lowest-order solution φ_0 and integrating, there follows

$$H(\psi) = \frac{\pi}{2}(1-v_0)\Theta(\psi - w^2/2)\int_{w^2/2}^{\psi} \frac{\mathrm{d}\hat{\psi}}{\sqrt{2\hat{\psi}}\,E(w^2/2\hat{\psi})},$$

where Θ is the unit step (Heaviside) function and E is the complete elliptic integral of the second kind. Far from the island, for $w^2 \ll \psi \ll 1$, $H(\psi)$ takes the asymptotic form

$$H(\psi) \sim (1-v_0)\left(\sqrt{2\psi} + \delta h\, w + O(w/\sqrt{\psi})\right),$$

where δh is a numerical constant defined by

$$\delta h = -1 + \int_1^\infty \frac{\mathrm{d}\Psi}{2\sqrt{\Psi}}\left(\frac{\pi}{2E(1/\Psi)} - 1\right) \simeq -0.69.$$

Note that this matches the small-x limit of the solution in the outer region with $\delta H_\infty = (1-v_0)\delta h$.

It follows from the above solution that at large distances from the island, the force required to pull the plasma through an island at velocity v_0 is

$$F_y = \mu \lim_{x\to\infty} \partial_x^2 \varphi = -0.69 D(v_0-1)w. \tag{30}$$

The natural island velocity (the velocity of the island in the absence of force, measured in the plasma frame) is thus equal to the electron diamagnetic velocity, $\omega = -v_{\mathrm{free}} = -1$.

Equation (30) shows that the force required to drag an island through the plasma at a velocity different from the natural velocity is proportional to the product of the particle diffusion coefficient D, the island width w and the difference between the island velocity and the natural velocity. Note that the above result leads to the surprising conclusion that the force F_y depends on the diffusivity D rather than the viscosity. This is a manifestation of the importance of the modifications of the density profile to the behaviour of magnetic islands.

Lastly, we may evaluate the effect of the polarization current on the island amplitude by substituting the result for $H'(\psi)$, equation (29), into the matching relation (19). After including the contribution of the outer (inertial) layer, we find

$$\hat{\Delta}_{\rm pol} = v_0(v_0 - 1)\left(\frac{0.4}{w} + \frac{\pi^2}{2\rho}\right).$$

We see that the right-hand side vanishes for $v_0 = 1$, the free propagation solution. It follows that the polarization current has no effect on the island amplitude for $Le = 0$.

4.3.2. General case. The general asymptotic form of the H profile for $x \gg w$ is $H(\psi) \sim H(x^2/2) \sim (1 - v_0)x + \delta H_\infty(v_0)$, where

$$\delta H_\infty(v_0) \equiv (v_0 - 1)w + \int_{w^2/2}^{\infty} {\rm d}\psi \left(\frac{{\rm d}H}{{\rm d}\psi} - \frac{1 - v_0}{\sqrt{2\psi}}\right) \tag{31}$$

represents the asymptotic shift in $H = n - \varphi$ with respect to the reference value $(1 - v_0)x$. The shift $\delta H_\infty(v_0)$ may be understood as resulting from the condition that H must be flat inside the island in order to satisfy the parallel force balance for the electrons. This accounts for a shift in H proportional to $(1 - v_0)w$ as found in equation (30). In the presence of a temperature gradient, however, there is an additional profile modification outside the island due to the effect of the thermal force. This effect is represented by the term proportional to $\eta_{\rm e}$ in the expression for H' given in equation (14).

Inspection of equation (14) reveals that H' is the sum of two terms proportional to the quantities $1 - v_0$ and $\eta_{\rm e}$ and that these quantities multiply coefficients that depend on Fz and v_0 only through the ratio $\Psi_{v_0} = v_0\sqrt{Le}/Fz^2$. We exploit these features by separating the integral in equation (31) according to

$$\delta H_\infty(v_0) = w[(1 - v_0)h_a(v_0^2\, Le/Fz^4) + \hat{\alpha}\,\eta_{\rm e} h_b(v_0^2\, Le/Fz^4)], \tag{32}$$

where

$$h_a(\Psi_{v_0}^2) = -1 + \int_1^{\infty} \frac{{\rm d}\Psi}{2\sqrt{\Psi}} \left(\frac{\hat{\Gamma}(\Psi, \Psi_{v_0})}{\Lambda(\Psi, \Psi_{v_0})} - 1\right), \tag{33}$$

$$h_b(\Psi_{v_0}^2) = \int_1^{\infty} \frac{{\rm d}\Psi}{2\sqrt{\Psi}} \frac{\Psi_{v_0}^2 \hat{\Upsilon}(\Psi)}{\Lambda(\Psi, \Psi_{v_0})}. \tag{34}$$

Here,

$$\Lambda(\Psi, \Psi_{v_0}) = \left(\hat{\Gamma} + \tfrac{2}{3}\hat{\alpha}^2\Psi_{v_0}^2\,\hat{\Upsilon}\right) 2E(1/\Psi)/\pi + \hat{\kappa}\Psi_{v_0}^2\,\hat{\Upsilon}\hat{\Gamma},$$

$$\hat{\Gamma}(\Psi, \Psi_{v_0}) = 2E(1/\Psi)/\pi + \Psi_{v_0}^2\,\hat{\Upsilon}/\,Le,$$

$$\hat{\Upsilon}(\Psi) = 2E(1/\Psi)/\pi - \pi/2K(1/\Psi)$$

and K is the complete elliptic integral of the first kind.

In addition to evaluating the integrals $h_a(\Psi_{v_0}^2)$ and $h_b(\Psi_{v_0}^2)$ numerically, we have found it useful to evaluate these integrals asymptotically for large Ψ_{v_0}. We present the asymptotic

analysis in the appendix, where we also describe a uniform approximation constructed by patching together the asymptotic expansion and the lowest-order Taylor expansion of the integrals for small v_0. We find that this uniform approximation gives good results over the entire range of the argument v_0 and for a wide range of values of the parameters.

Lastly we describe the evaluation of the integral of the polarization current. From the equilibrium result $j = -H'(\psi)\tilde{\varphi}$, we see that the integrand of equation (20) is proportional to the cold-electron stream velocity $\partial_x H = xH'$. Similarly to the force integral we make the dependence on η_e explicit by separating the integral into two parts according to

$$\hat{\Delta}_{\rm pol}(v_0) = \frac{v_0}{w}[(1-v_0)\delta_a(v_0^2\, Le/Fz^4) + \hat{\alpha}\,\eta_e\delta_b(v_0^2\, Le/Fz^4)], \tag{35}$$

where

$$\delta_a(\Psi_{v_0}) = 8\int_1^\infty \frac{{\rm d}\Psi}{\sqrt{\Psi}}\,\frac{\hat{\Gamma}(\Psi,\Psi_{v_0})}{\Lambda(\Psi,\Psi_{v_0})}\,J_R(\Psi), \tag{36}$$

$$\delta_b(\Psi_{v_0}) = 8\int_1^\infty \frac{{\rm d}\Psi}{\sqrt{\Psi}}\,\frac{\Psi_{v_0}\hat{\Upsilon}(\Psi)}{\Lambda(\Psi,\Psi_{v_0})}\,J_R(\Psi). \tag{37}$$

with

$$J_R(\Psi) = \frac{\langle\cos y\rangle_\psi}{\langle 1\rangle_\psi} = 1 - 2\Psi[1 - E(1/\Psi)/K(1/\Psi)].$$

The above analytic forms for the polarization integral are compared with the numerical results from the IslET code in figure 4. We present in the appendix a uniform approximation to the polarization integral calculated by patching together the asymptotic results for large and small arguments in a similar way as for the force integrals. The uniform approximation is compared with the exact integrals in figure 5.

This completes the analytic solution of the nonlinear equilibrium and transport equations in the unmagnetized regime $w \ll 1$. We next turn to the examination and interpretation of the results.

4.3.3. Slip curves and natural velocity. The force needed to drag the island through the plasma at velocity v_0 is

$$F_y = \mu \lim_{x\to\infty} \partial_x^2\varphi = D\,w[(1-v_0)h_a(v_0^2\, Le/Fz^4) + \hat{\alpha}\,\eta_e h_b(v_0^2\, Le/Fz^4)]. \tag{38}$$

Figure 4 compares the slip curves deduced by numerical evaluation of the integrals in equation (38) with the solutions of the IslET code for three different values of the island width. The figure shows that the thin-island limit is surprisingly good even for values of w of order unity.

It is important to note that for $Sc \sim 1$, the magnitude of the velocity gradient $U \simeq v_y'$ is needed so that $v_0 - v_{\rm free} \sim v_{\rm free}$ is itself of order unity. In the core of magnetic confinement experiment, however, the velocity gradient is typically weak on the scale of the island, in the sense that $W/L_T \ll 1$. Thus, the plasma velocity near islands located in the core will be very close to the natural velocity, $v_0 \simeq v_{\rm free}$, even in the presence of external forces such as those exerted by error fields or image currents in external structures. For such islands the slip curves derived here may be viewed as an analytic device for illuminating the freely and almost freely propagating solutions, in the same way that complex analysis sheds light on the behaviour of real functions. Note that the theory of mode locking is based on the assumption that $v_0 \simeq v_{\rm free}$. Our results show that this assumption is justified even in the presence of plasma inhomogeneity.

Near the edge of the plasma, by contrast, strong velocity gradients are commonly observed even in the absence of any island. The slip curves may thus be relevant to the interpretation of

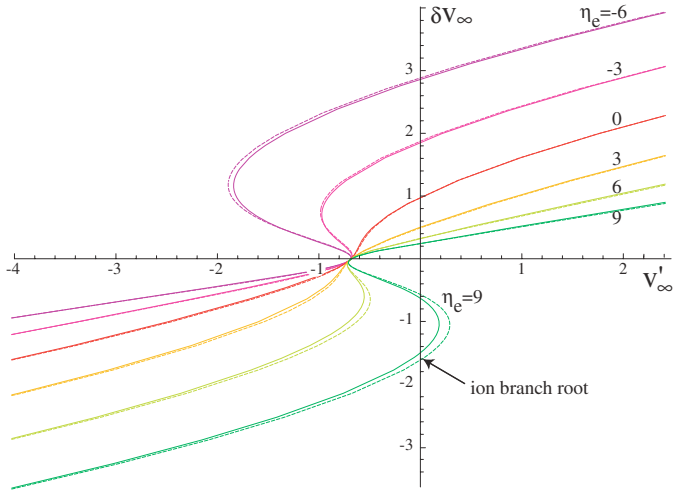

Figure 5. Slip velocity v_∞ as a function of the applied force, proportional to v'_∞, for values of η_e ranging from -6 to 9 in steps of 3. The solid lines show the result of evaluating the force integral in equations (32)–(34) numerically and the dashed lines show the uniform analytic approximation given in equations (48)–(49) of the appendix. The parameters are $Sc = 1$, $Le = 4.0$ and $Fz = 0.7$.

velocity profiles in edge islands, such as those used in island divertors. The model used here, however, does not contain the physical effects that are responsible for the strong edge velocity gradients found in the absence of an island. Reference [8] gives experimental profiles of the velocity across an island in the edge of the LHD stellarator. The large velocity gradients and their modification as the island size increases are evident.

Figure 5 compares a family of slip curves computed in two ways: first (solid lines) by numerically evaluating the integrals in equation (38) and second (dashed lines) by using the uniform analytic approximation described by equations (46)–(49). The curves in this plot correspond to a sequence of values of η_e ranging from -6 to 9 in steps of 3. For large values of η_e and small values of Fz and Le, the slip curves exhibit hysteresis. When the hysteresis is sufficiently pronounced it results in the birth of secondary solution branches corresponding to islands propagating in the ion direction, as shown in figure 4 by the three intersections of the slip curve for $\eta_e = 9$ with the ordinate. The existence of multiple solution branches has been pointed out previously by Ottaviani *et al* [38]. The simulations of [38], however, assumed isothermal conditions so that it is likely that their solution branches are unrelated to the ion branch predicted here. In fact, the existence of the ion branch requires that η_e, Le and Fz^{-4} take unusually large values. Large values of η_e may occur in H-mode discharges where the density gradient can be very small, but the small values of Fz^{-4} resulting from anomalous transport make the emergence of an ion branch unlikely.

In principle one may determine the natural velocity by solving equation (38) for v_{free} such that $F_y = 0$. Due to the particular form of F_y, however, it is more convenient to solve instead for η_e such that $F_y = 0$:

$$\eta_e = \frac{(v_{\text{free}} - 1)}{\hat{\alpha}} \frac{h_a(v_{\text{free}}^2\, Le/Fz^4)}{h_b(v_{\text{free}}^2\, Le/Fz^4)}.$$

This result defines the natural propagation velocity implicitly in terms of η_e and is shown in figure 6 for $Le = 5.0$ and a sequence of Fz values described by $Fz = 2^{j/2}$, where $j = -2, \ldots, 2$. We see that the propagation velocity is a decreasing function of η_e, in contrast

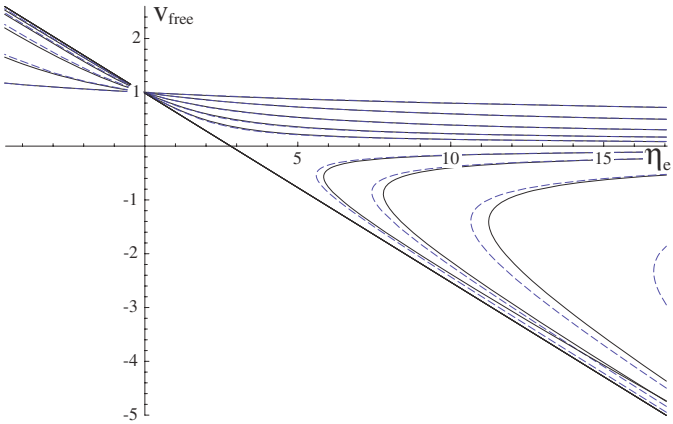

Figure 6. Natural velocity as a function of the electron temperature gradient parameter η_e. The solid lines show the result of evaluating the force integral in equations (32)–(34) numerically and the dashed lines show the uniform analytic approximation given in equations (48)–(49) of the appendix. The parameters are $Sc = 1$, $Le = 5.0$ and $Fz = 2^{j/2}$ with $j = -4, \ldots 4$.

with the linear result, equation (27). In the lower half-plane figure 6 shows the variation of the natural velocity for the ion roots that we identified earlier in figure 6. The large values of η_e required for the existence of these ion roots are evident here. Lastly, we recall that the constant-v_0 approximation fails when v_0 is small, so that the asymptote corresponding to the limit $v_{free} \to 0$ as $\eta_e \to \infty$ may be an artefact of this approximation. Unfortunately, the IslET code fails to converge in this limit, so that we are unable to determine the correct solution for $v_0 \ll 1$.

In order to gain a physical understanding of the processes determining the natural velocity, we examine the limit $Le/Fz^4 \to \infty$ corresponding to small perpendicular particle diffusivity. This limit allows an asymptotic analysis that is described in the appendix. The result is

$$v_{free} = 1 - \eta_e/\eta_{ec}(Le), \tag{39}$$

where

$$\eta_{ec}(Le) = \frac{1}{\hat{\alpha}} \frac{h_{a\infty}(Le)}{h_{b\infty}(Le)} \tag{40}$$

represents the value of η_e such that the propagation reverses direction. Here the $h_{s\infty}(Le)$ are algebraic functions of Le given in the appendix ($s = a, b$). Figure 7 shows the function $\eta_{ec}(Le)$ along with the following Padé approximation valid for large Le:

$$\eta_{ec}(Le) \simeq \eta_{ec\infty} \left(1 - \frac{(\hat{\kappa}/Le)^{1/4}}{(\hat{\kappa} + \frac{2}{3}\hat{\alpha}^2)^{1/2}} \right)^{-1}, \tag{41}$$

where

$$\eta_{ec\infty} \equiv \lim_{Le\to\infty} \eta_{ec}(Le) = \frac{\hat{\kappa}}{\hat{\alpha}} + \frac{2}{3}\hat{\alpha}. \tag{42}$$

In the limit $Le \to \infty$ corresponding to large perpendicular heat diffusivity, we recover the result of Connor *et al* [28]. We note, however, that when the particle and perpendicular heat diffusivities are both neglected as in [23], the natural velocity is indeterminate. The natural velocity depends sensitively on its argument, in fact, varying with the one-fourth power of Le for large Le. This shows that the particle diffusivity is important even when it is very small.

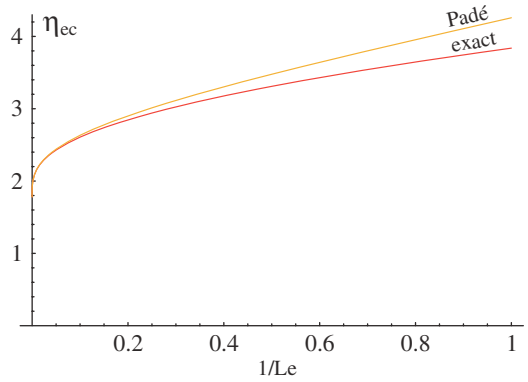

Figure 7. Critical η_e as a function of Le^{-1} for propagation reversal in the limit of large Le/Fz^4.

The singular nature of the limit $Le \to \infty$ results from the fact that thermal effects on the cold-electron streamfunction H depend on parallel heat and particle fluxes that are mediated by the polarization current and thus are localized very close to the separatrix. In mathematical terms, Υ decays rapidly whereas $\langle \partial^\psi \varphi \rangle_\psi$ reaches a constant value far from the island.

The $Le \to \infty$ limit is helpful, however, for gaining insight into the role of the electron temperature gradient. Of particular interest is the unexpected inverse variation of the island propagation velocity with η_e. There are two reasons why one might expect the velocity to increase with η_e. First, the electrons immediately *outside* the separatrix are drifting at velocity $v > 1$ when $\eta_e > 0$, and one might expect the island to adjust its speed so as to propagate with these neighbouring electrons. Second, there is always a small residual electron temperature gradient *inside* the separatrix that should cause the island to propagate with $v > 1$ by virtue of the frozen-in property of the electrons.

The reason for the reduction in the island propagation velocity with increasing η_e lies in the balance between particle and heat transports. To see this, consider the limit $\kappa_\parallel \to \infty$ such that $T = T(\psi)$. From the continuity equation with $D = 0$, we find

$$v_E \cdot \nabla n = \nabla_\parallel j,$$

indicating that the convective particle flux across the flux surfaces must balance the convective parallel flux caused by the polarization current. Omitting the parallel heat conduction for simplicity, the heat equation takes the similar form

$$v_E \cdot \nabla T = \tfrac{2}{3}\hat{\alpha} T \nabla_\parallel j \quad \text{and}$$

eliminating the current leads to

$$\tfrac{2}{3}\hat{\alpha}\, v_E \cdot \nabla n = v_E \cdot \nabla \log T. \tag{43}$$

Using the equilibrium properties $T = T(\psi)$ and $n = \varphi + H(\psi)$, we find $\eta_e \nabla_\parallel \varphi = \tfrac{2}{3}\hat{\alpha} H' \nabla_\parallel \varphi$, whence $H' = 3\eta_e/2\hat{\alpha}$. For $w \ll x \ll 1$, it follows that

$$v_{\text{free}} = 1 - \frac{3}{2}\frac{\eta_e}{\hat{\alpha}}.$$

We recover the $\kappa \ll 1$ limit of equations (39)–(42). Thus, we see that the natural velocity is set by the requirement that the parallel electron flow balances the perpendicular fluxes of both heat and particles. In the case of a constant-temperature island with diamagnetic propagation, $\omega = 1$, the convective particle flux vanishes (since the electrons are at rest in the island frame). If a small electron temperature gradient is imposed, the particle flux must increase to maintain

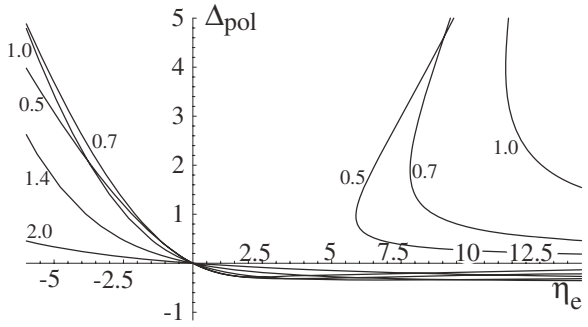

Figure 8. Polarization integral as a function of η_e for $Fz = 2^{j/2}$, $j = -2, \ldots 2$. The other parameters are $Sc = 1$ and $Le = 5.0$.

the balance in equation (43). This requires that the island slows down in order to create an electron flux in the electron diamagnetic direction.

We conclude by examining the dependence of the polarization integral on η_e. Figure 8 shows a parametric plot of Δ_{pol} versus η_e. This plot summarizes the effect of the electron temperature gradient on a freely propagating island. It shows that the polarization current is strongly destabilizing when the electron temperature gradient is opposite to the density gradient, $\eta_e < 0$, a condition that may occur in some beam-heated H-mode discharges. For $\eta_e > 0$, by contrast, the polarization current is stabilizing for the standard electron branch solution. When it exists, the ion branch always suffers a destabilizing effect from the polarization current. As discussed above, however, it is unlikely that the transport parameters are such so as to allow the ion branch to exist for the parameters normally encountered in experiments.

5. Discussion

The stability of magnetic islands is profoundly affected by polarization effects when the parameter $\hat{\beta}/\rho_s = (\beta/\rho_s)(L_s^2/L_n^2)$ is large. We have investigated the propagation velocity and the growth of islands in the *unmagnetized* regime ($W \ll \rho_s$). We find that when the electron temperature gradient parameter η_e is positive, the island propagates more slowly than the electron drift speed, resulting in a stabilizing effect. The reduction in propagation velocity with increasing electron temperature gradient is a consequence of the equilibration between convective particle and heat fluxes, both of which are balanced by the same parallel current. Our results also show that particle diffusion (collisional or anomalous) plays an important role by inhibiting the flattening of the density inside the separatrix. The sensitivity to the diffusion coefficient is exhibited by the dependence of the propagation velocity on the one-fourth power of the Lewis number.

Our analysis suggests an explanation for the discrepancies between the numerical results obtained by previous authors. These numerical results are consistent with the fact that profile flattening by parallel electron transport is a quasilinear effect that becomes ineffective in the nonlinear regime $W \gg W_\parallel$. In particular, Biskamps's results appear to be a consequence of his use of a single harmonic [39]. This prohibits the alignment of certain quantities which is an important feature of the nonlinear solution. For example, the electron stream function $n - \varphi$ must be constant along flux surfaces, but the vanishing of $\nabla_\parallel(n - \varphi)$ is impossible if a single harmonic is used [28]. That is, the use of a single harmonic effectively enforces quasilinear

dynamics even in the regime $W \gg W_\parallel$ corresponding to the very large magnetic Reynolds numbers ($S = 10^6$) that Biskamp used [39].

Monticello and White, by contrast, used an adequate number of harmonics and found that islands initialized with an amplitude greater than the conduction channel width continued growing while propagating at nearly the electron drift velocity. They found that profile flattening occurred only if the island was initialized in the quasilinear regime where $W \sim W_\parallel$. They also pointed out that the nonlinear regime required using a rather high magnetic Reynolds number of $S = 1.25 \times 10^5$, while they observed profile flattening for $S = 10^4$. Scott *et al* [42] confirmed the results of Monticello and White and calculated numerically the curve separating the quasilinear from the fully nonlinear regime.

More recently, Ottaviani *et al* [38] examined parameters such that $0.2 < C = \hat{\beta}^{1/2} < 2$. For the smaller values of $C = \hat{\beta}^{1/2}$ lying in the semi-collisional, constant-$\tilde{\psi}$ regime, they found two types of solutions: a thin island propagating at the drift velocity and a wider island propagating very slowly in the electron diamagnetic direction. The properties of the thin-island solutions are consistent with the results of the present paper. The wide-island solutions, by contrast, are magnetized ($W > \rho_s$) and so fall outside the scope of the present paper. We note, however, that since we have shown that parallel transport does not flatten the density for $C^{1/2}\rho_s \ll W \ll \rho_s$, it is unclear why it would flatten the density in the magnetized regime. An alternative explanation for the density flattening observed for magnetized islands in [38] is that it is caused by the excitation of drift waves. Note that the parameters used in the present paper are related to those of [38, 43] by $C = \eta v_*/\rho_*^4$, $\hat{\beta}^{1/2} = v_*/\rho_*$ and $\hat{\Delta} = \Delta'\rho_*^3/v_*^2$. In terms of the parameters of [38], our neglect of parallel ion compressibility is justified when $w^2\beta \ll v_*^2$.

Lastly, Fitzpatrick and coworkers [43] have examined both the propagation and the growth of magnetic islands using the same model as Ottaviani *et al* [38]. Instead of varying v_*, however, they varied $w = W/\rho_s$ from 0.4 to 1000 in such a way that $\hat{\beta} = C^{1/2} = w^2$. For $w < 1$ the results of [43] show that there is no flattening and $\omega \simeq \omega_*$, even though the islands satisfy $\omega_* \ll k_\parallel^2 D_\parallel$. This is consistent with the findings of the present paper and confirms that parallel transport does not flatten the density of freely propagating islands in the absence of an electron temperature gradient. Note that in the case of forced propagation, corresponding to islands locked to an externally driven field asymmetry (such as an error field) or islands in a stellarator, parallel transport will cause the density to either steepen or flatten when the island is made to propagate, respectively, faster or slower than the background diamagnetic frequency. This serves to achieve parallel force balance inside the separatrix.

Our conclusions regarding density flattening can be summarized as follows. Outside the conduction channel, parallel transport ensures that the density responds adiabatically to electrostatic perturbations. For unmagnetized islands in the semi-collisional regime, parallel transport does *not* flatten the density of freely propagating islands when the island width exceeds the width of the conduction channel. Convection cells, by contrast, may provide a mechanism for density profile modification that is effective in the non-compressive regime, $W < W_a$. For $W \ll \rho_s$, however, our analysis argues against the existence of secondary solutions exhibiting convection cells.

Acknowledgments

The author acknowledges helpful discussions with R Fitzpatrick, A Hassam, F Militello and M Ottaviani. This work was funded by the US DoE Contract No DE-FG03-96ER-54346 and by the Center for Multiscale Plasma Dynamics under Contract No DE-FC02-04ER54785.

Appendix A. Asymptotic forms of the force and polarization integrals

In this appendix we derive an asymptotic expression for the two integrals describing the dependence of the force applied on the island and of the polarization current on the quantity $\Psi_{v_0} = v_0\sqrt{Le}/\mathrm{Fz}^2$.

The asymptotic analysis of the functions $h_a(\Psi_{v_0}^2)$ and $h_b(\Psi_{v_0}^2)$ proceeds by noticing that the function $\Upsilon(\Psi)$ describing the polarization effect decreases much faster at large Ψ than $\Gamma(\Psi)$ or $E(1/\Psi)$. Specifically,

$$E(\Psi^{-1}) \sim \pi/2,$$
$$\hat{\Upsilon}(\Psi) \sim \Psi^{-2}/32.$$

It follows that the dominant contribution to the integral comes from the region $\Psi \sim \Psi_{v_0} \gg 1$. The integral may thus be evaluated by expanding its argument for large Ψ, changing variables to $p = 32(\Psi/\Psi_{v_0})^2$ and subsequently keeping only lowest-order terms in $1/\Psi_{v_0}$. We find

$$h_s(\Psi_{v_0}^2) \sim h_{s\infty}(Le)\,(\Psi_{v_0}/4\sqrt{2})^{1/2}, \tag{44}$$

where $s = a, b$ and

$$h_{a\infty}(\Psi_{v_0}) = \int_0^\infty \mathrm{d}p\,\frac{(p + 1/Le)p^{1/4}}{4Q(p)},$$
$$h_{b\infty}(\Psi_{v_0}) = \int_0^\infty \mathrm{d}p\,\frac{p^{1/4}}{4Q(p)}.$$

Here

$$Q(p) = p^2 + \left[\tfrac{2}{3}\hat{\alpha}^2 + \hat{\kappa} + 1/Le\right]p + \hat{\kappa}/Le. \tag{45}$$

We note that for $Le = 1$, the integrand in $h_{a\infty} + h_{b\infty}$ is proportional to the conductivity $\hat{\sigma}(s)$ found in equation (24) for the linear regime. This proportionality is probably coincidental, however, since the physical processes described by H' and σ and the transverse scale on which they vary are very different. In particular, the effect of perpendicular transport is neglected in the derivation of σ.

The integrals are easily evaluated by using the method of residues. There follows

$$h_{a\infty}(Le) = \frac{\pi}{2\sqrt{2}}\frac{(1/Le - p_+)(-p_+)^{1/4} - (1/Le - p_-)(-p_-)^{1/4}}{p_+ - p_-}, \tag{46}$$

$$h_{b\infty}(Le) = \frac{\pi}{2\sqrt{2}}\frac{(-p_+)^{1/4} - (-p_-)^{1/4}}{p_+ - p_-}, \tag{47}$$

where the $p_\pm$ are the roots of $Q(p) = 0$.

The applicability of the asymptotic formulae can be extended to a finite value of the argument by connecting them to the Taylor expansion of the integrals for small Ψ_{v_0}. Numerical evaluation yields $h_a(0) = -0.69$ and $h_b'(0) = 0.076$. Combining the Taylor and asymptotic expansion yields the following approximation:

$$h_a(\Psi_{v_0}^2) = \tfrac{1}{2}h_{a\infty}(Le)[(2h_a(0)/h_{a\infty}(Le))^4 + \Psi_{v_0}^2/2]^{1/4}, \tag{48}$$

$$h_b(\Psi_{v_0}^2) = h_{b\infty}(Le)\frac{\Psi_{v_0}^2}{4}\left[h_{b\infty}(Le)/(4h_b'(0)) + (\Psi_{v_0}^2/2)^{3/4}\right]^{-1}, \tag{49}$$

where we have adjusted the exponents of the various terms to yield the best fit consistent with the limits of large and small v_0. The above expressions provide a good uniform approximation

to the force integrals over the entire range of parameters. Figure X compares the exact integrals and the uniform approximations shown above.

We may evaluate the polarization integral using the same approach. For large Ψ, $J_R(\psi) \sim 1/8\Psi$. The asymptotic evaluation of the $\delta_s(\Psi_{v_0})$ leads to

$$\delta_s(\Psi_{v_0}) \sim \delta_{s\infty}(Le)\,(\Psi_{v_0}/4\sqrt{2})^{-1/2}, \tag{50}$$

where

$$\delta_{a\infty}(Le) = \frac{\pi}{\sqrt{2}}\frac{(1/Le - p_+)(-p_+)^{-1/4} - (1/Le - p_-)(-p_-)^{-1/4}}{p_+ - p_-}, \tag{51}$$

$$\delta_{b\infty}(Le) = \frac{\pi}{\sqrt{2}}\frac{(-p_+)^{-1/4} - (-p_-)^{-1/4}}{p_+ - p_-}. \tag{52}$$

Combining the asymptotic results with the Taylor expansions for small v_0 yields the uniform approximations

$$\delta_a(\Psi_{v_0}) = 2\delta_{a\infty}(Le)[(2\delta_{a\infty}(Le)/\delta_a(0))^3 + (\Psi_{v_0}^2/2)^{3/4}]^{-1/3}, \tag{53}$$

$$\delta_b(\Psi_{v_0}) = \delta_{b\infty}(Le)\Psi_{v_0}^2\left[(\delta_{b\infty}(Le)/(\delta_b'(0)))^{1/2} + (\Psi_{v_0}^2/2)^{5/8}\right]^{-2}. \tag{54}$$

The uniform approximation given above is compared with the numerically evaluated integrals in figure 8.

References

[1] Chapman B E, Fitzpatrick R, Craig D, P M and Spizzo G 2004 **11** 2156
[2] Escande D F *et al* 2000 *Phys. Rev. Lett.* **85** 1662
[3] Franz P *et al* 2004 *Phys. Rev. Lett.* **92** 125001
[4] Franz P *et al* 2006 *Phys. Plasmas* **13** 012510
[5] Spizzo G *et al* 2006 *Phys. Rev. Lett.* **96** 025001
[6] Jaenicke R *et al* 1993 *Nucl. Fusion* **33** 687
[7] Wagner F 2005 *Phys. Plasmas* **12** 072509
[8] Ida K *et al* 2002 *Phys. Rev. Lett.* **88** 015002
[9] Tanaka K *et al* 2002 *Plasma Phys. Control. Fusion* **44** A231
[10] Inagaki S *et al* 2004 *Phys. Rev. Lett.* **92** 055002
[11] Ida K *et al* 2004 *Plasma Phys. Control. Fusion* **44** 290
[12] de Vries P C *et al* 1997 *Nucl. Fusion* **37** 1641
[13] Taylor E D *et al* 2002 *Phys. Plasmas* **9** 3938
[14] Severo J H F *et al* 2004 *Phys. Plasmas* **11** 846
[15] de Vries P C *et al* 1997 *Plasma Phys. Control. Fusion* **39** 439
[16] Chang Z Y *et al* 1994 *Nucl. Fusion* **34** 1309
[17] Coppi B, Mark S L and Bertin G 1979 *Phys. Rev. Lett.* **42** 1058
[18] Chang C S, Dominguez R R and Hazeltine R D 1981 *Phys. Fluids* **24** 1655
[19] Drake J F, Antonsen J T M, Hassam A B and Gladd N T 1983 *Phys. Fluids* **26** 2509
[20] Sauter O *et al* 1997 *Phys. Plasmas* **4** 1654
[21] Lahaye R *et al* 2006 *Phys. Plasmas* **13**
[22] Narihara K *et al* 2001 *Phys. Rev. Lett.* **87** 135002
[23] Smolyakov A I 1993 *Plasma Phys. Control. Fusion* **35** 657
[24] Wilson H R, Connor J W, Hastie R J and Hegna C C 1996 *Phys. Plasmas* **3** 248
[25] Waelbroeck F L and Fitzpatrick R 1997 *Phys. Rev. Lett.* **78** 1703
[26] Mikhailovskii A B, Pustovitov V D, Smolyakov A I and Tsypin V S 2000 **7** 1214
[27] Mikhailovskii A B, Tsypin V S, Nascimento I C and Galvao R M O 2000 *Phys. Plasmas* **7** 3474
[28] Connor J W, Waelbroeck F L and Wilson H R 2001 *Phys. Plasmas* **8** 2835
[29] Waelbroeck F L, Connor J W and Wilson H R 2001 *Phys. Rev. Lett.* **87** 215003
[30] Poli E, A P and Bergman A G 2005 *Phys. Rev. Lett.* **94** 205001
[31] Poli E *et al* 2005 *Nucl. Fusion* **45** 384
[32] Bergmann A, Poli E and Peeters A G 2005 *Phys. Plasmas* **12** 072501

[33] Mikhailovskii A B, Konovalov S V and Pustovitov V D 2000 *Phys. Plasmas* **7** 2530
[34] Fitzpatrick R and Waelbroeck F L 2004 *Phys. Fluids* **12**
[35] Fitzpatrick R and Waelbroeck F L 2005 *Phys. Plasmas* **12** 22308
[36] Fitzpatrick R, Watson P and Waelbroeck F L 2005 *Phys. Plasmas* **12** 082510
[37] Scott B D, Hassam A B and Drake J F 1985 *Phys. Fluids* **28** 275
[38] Ottaviani M, Porcelli F and Grasso D 2004 *Phys. Rev. Lett.* **93** 075001
[39] Biskamp D 1979 *Nucl. Fusion* **19** 777
[40] Hicks H R, Carreras B A and Holmes J A 1984 *Phys. Fluids* **27** 909
[41] Monticello D A and White R B 1980 *Phys. Fluids* **23** 366
[42] Scott B D and Hassam A B 1987 *Phys. Fluids* **30** 90
[43] Fitzpatrick R, Waelbroeck F L and Militello F 2006 *Phys. Plasmas* **13** 122507
[44] Yu and Brower D 1992 *Nucl. Fusion* **32** 1545
[45] Hender T C *et al* 1992 *Nucl. Fusion* **32** 2091
[46] McCool S *et al* 1990 *J. Nucl. Mater.* **176–177** 716
[47] Van Milligen B P *et al* 1993 *Nucl. Fusion* **33** 1118
[48] Navratil G A *et al* 1998 *Phys. Plasmas* **1998** 1855
[49] La Haye R J, Petty C C, Strait E J, Waelbroeck F L and Wilson H R 2003 *Phys. Plasmas* **10** 3644
[50] Waelbroeck F L 2005 *Phys. Rev. Lett.* **95** 035002
[51] Fitzpatrick R 1995 *Phys. Plasmas* **2** 825
[52] Militello F, Hastie R J and Porcelli F 2006 *Phys. Plasmas* **13** 112512
[53] Arcis N, Escande D F and Ottaviani M 2006 *Phys. Plasmas* **13** 052305
[54] Fitzpatrick R and Waelbroeck F 2005 *Phys. Plasmas* **12** 122511